Cogn Neurodyn (2016) 10:211–223
DOI 10.1007/s11571-015-9374-9

RESEARCH ARTICLE

Temporal properties of dual-peak responses of mouse retinal ganglion cells and effects of inhibitory pathways

Ru-Jia Yan[1] · Hai-Qing Gong[1] · Pu-Ming Zhang[1] · Shi-Gang He[1] · Pei-Ji Liang[1]

Received: 19 June 2015 / Revised: 8 December 2015 / Accepted: 24 December 2015 / Published online: 19 February 2016

Abstract Dual-peak responses of retinal ganglion cells (RGCs) are observed in various species, previous researches suggested that both response peaks were involved in retinal information coding. In the present study, we investigated the temporal properties of the dual-peak responses recorded in mouse RGCs elicited by spatially homogeneous light flashes and the effect of the inhibitory inputs mediated by GABAergic and/or glycinergic pathways. We found that the two peaks in the dual-peak responses exhibited distinct temporal dynamics, similar to that of short-latency and long-latency single-peak responses respectively. Pharmacological studies demonstrated that the application of exogenous GABA or glycine greatly suppressed or even eliminated the second peak of the cells' firing activities, while little change was induced in the first peak. Co-application of glycine and GABA led to complete elimination of the second peak. Moreover, application of picrotoxin or strychnine induced dual-peak responses in some cells with transient responses by unmasking a second response phase. These results suggest that both GABAergic and glycinergic pathways are involved in the dual-peak responses of the mouse RGCs, and the two response peaks may arise from distinct pathways that would converge on the ganglion cells.

Keywords Retinal ganglion cell · Dual-peak response · Temporal property · Inhibitory pathway

✉ Pei-Ji Liang
pjliang.nip@gmail.com; pjliang@sjtu.edu.cn

[1] School of Biomedical Engineering, Shanghai Jiao Tong University, 800 Dong-Chuan Road, Shanghai 200240, China

Introduction

In vertebrate retinas, retinal ganglion cells (RGCs) are the output neurons where visual information is encoded in spikes and further transmitted to the central visual system (Masland 2001; Wässle 2004). Various activity patterns can be observed in RGCs' light responses (Cleland and Levick 1974; Nirenberg and Meister 1997; Farrow and Masland 2011). In response to spatially uniform light flashes, RGCs show various firing patterns with different temporal properties. While some RGCs exhibit sustained firings, others respond with very transient bursts of spikes; at the meantime, some respond rapidly at the stimulus onset while others respond with relatively longer latencies (Hamasaki and Winters 1974; Soucy et al. 1998; Awatramani and Slaughter 2000; Carcieri et al. 2003; Xu et al. 2005). Besides, another response pattern exhibiting two peaks in peri-stimulus time histogram (PSTH) has also been reported, which is referred to as dual-peak response (Soucy et al. 1998; Thiel et al. 2006; Zhou et al. 2007).

It was previously suggested that both response peaks in dual-peak pattern contributed to retinal information coding. In turtle RGCs, dual-peak response pattern was observed when the retina was stimulated by spatially homogeneous light flashes with pseudo-random intensity steps, and stimulation intensities were better discriminated when the properties of both response peaks were considered (Greschner et al. 2006). This implied that both peaks in the dual-peak response carried information about the stimuli.

The origin of the dual-peak response has also been investigated. Two hypotheses have been proposed. The first one assumes that the two peaks in the PSTH may originate from distinct pathways, with the first peak being generated from the direct photoreceptor—bipolar cell—ganglion cell pathway, and the second peak being related to a more

complex neuronal circuitry involving amacrine cell network (Nirenberg and Meister 1997; Dong and Werblin 1998; Popova et al. 2003; Zhou et al. 2007). It has been documented that blockade of GABAergic pathway(s) could cause the appearance of a later component in some RGCs with transient responses, switching the response patterns from single-peak to dual-peak (Nirenberg and Meister 1997; Dong and Werblin 1998; Popova et al. 2003). This finding suggested that the generation of the second peak might be suppressed by GABAergic activity. However, the second hypothesis assumes that the dual-peak response might be shaped by a delayed inhibitory feedback from amacrine cells that truncated the sustained excitatory input to the ganglion cells, with the inhibitory process ended before the excitatory signal from bipolar cells was ceased, to allow for the second peak (Thiel et al. 2006). This hypothesis was supported by findings in turtle retina that pharmacologically blocking glycinergic pathway(s) resulted in the transformation from dual-peak pattern into single-peak pattern, suggesting that the inhibitory process might involve glycinergic inhibition (Thiel et al. 2006). Despite the differences in the two hypotheses, they both indicated that the shaping of the dual-peak responses of RGCs was related to the activity of inhibitory pathway(s).

GABA and glycine are both important inhibitory transmitters in retinas and are released by different types of amacrine cells (Wässle et al. 1998; Yang 2004; Shen and Jiang 2007). In mammals, approximately half of the amacrine cells are GABAergic, while the other half are glycinergic (Wässle et al. 2009; Werblin 2011). The aim of the present study was thus to investigate the potential contribution of the inhibitory input mediated by GABAergic and/or glycinergic pathway(s) to the dual-peak response pattern of mouse RGCs. Using spatially uniform light flashes, dual-peak and single-peak responses with different temporal patterns were observed in mouse RGCs. It was found that in the dual-peak responses, the temporal properties of the two peaks resembled those of short- and long-latency single-peak responses respectively. Pharmacological studies further revealed that when exogenous GABA or glycine was applied, the second response peak could be suppressed or even be eliminated, while little change was induced in the first peak. Co-application of GABA and glycine led to further suppression or even complete elimination of the second peak in the dual-peak responses. Moreover, blockade of GABAergic or glycinergic pathway(s) could induce the dual-peak responses in RGCs which had shown single-peak responses in control. These results suggest that the two response peaks of the dual-peak response in mouse RGCs involve separate mechanisms, and arise from distinct pathways that converge on the ganglion cells; the formation of dual-peak responses is dependent on the modulation of GABAergic and/or glycinergic pathways.

Materials and methods

Preparation

Adult (2–3 months) C57BL/6 wild-type mice were used in the present study. Mice were dark adapted for at least 30 min before the experiment and were killed by cervical dislocation under dim red light. The eyes were enucleated and the retinas were isolated in oxygenated (95 % O_2 and 5 % CO_2) Ringer's solution containing: 124.0 mM NaCl, 2.5 mM KCl, 1.3 mM NaH_2PO_4, 2.0 mM $CaCl_2$, 2.0 mM $MgCl_2$, 22.0 mM glucose and 26.0 mM $NaHCO_3$ (pH 7.4). A small piece of retina was cut from the periphery (about 3×3 mm^2) and then placed on a piece of nitrocellulose filter paper (0.22 μm pore size, White GSWP, Millipore Corporation, Bedford, MA, USA), with the photoreceptor side contacting the filter paper. The mounted retina was then transferred onto a multi-electrode array (MEA) which was connected to the recording system (MEA-System, Multi Channel Systems MCS GmbH, Reutlingen, Germany), the ganglion cell layer facing the electrodes. This preparation was continuously perfused with oxygenated Ringer's solution at 34–37 °C. In the pharmacological studies, GABA (250 μM), picrotoxin (40 μM), glycine (100 μM) and strychnine (5 μM) were applied with the Ringer's solution as desired (Nirenberg and Meister 1997; Protti et al. 1997; McCall et al. 2002; Toychiev et al. 2013; Ishii and Kaneda 2014). All drugs were purchased from Sigma-Aldrich (Saint Louis, MO, USA). All described procedures were reviewed and approved by Institutional Animal Care and Use Committee at Shanghai Jiao Tong University.

Electrophysiological recording

Ganglion cells' activities were recorded via a MEA, which consisted of 60 electrodes (10 μm in diameter) arranged in an 8×8 matrix (with the four corners vacant) with 100 μm tip-to-tip distance between adjacent electrodes (horizontally and vertically). The raw electrode data were amplified through a 60-channel amplifier (single-ended, amplification 1200×, amplifier input impedance $>10^{10}$ Ω, output impedance 330 Ω). Signals from each selected channel were sampled at a rate of 20 kHz (MC_Rack, Multi Channel Systems MCS GmbH) and stored in a computer. Timing signals of visual stimuli were also recorded and stored in the computer.

Spike sorting was performed using the method proposed by Zhang et al. (2004), as well as the spike-sorting unit in

the commercial software OfflineSorter (Plexon Inc., Dallas, TX, USA). Only single-neuron events clarified by both spike-sorting methods mentioned above were used for further analyses (Jing et al. 2010a; Zhang et al. 2014).

Visual stimulation

Light stimulus was generated from a computer monitor (Vision Master Pro 450, Iiyama, Japan) and was focused to form a 0.9×0.9 mm^2 image while projected onto the isolated retina through a lens system. Full-field sustained white light (10.4 nW/cm^2) was given for 30 s to adjust the sensitivity of the ganglion cells to similar levels before stimulation protocol was applied (Liu et al. 2007; Jing et al. 2010b). The stimulation protocol consisted of full-field light flashes with 1-s ON duration (20.8 nW/cm^2) and 1-s OFF interval (0 nW/cm^2), which was repeated for 100 times.

Measurement of latency, duration and peak firing rate of mouse RGC's response

Response latency, peak firing rate and response duration were measured following the method introduced by Carcieri et al. (2003). The PSTH of RGC's response was calculated, and was then smoothed by a non-parametric regression method Bayesian Adaptive Regression Splines (BARS) (Dimatteo et al. 2001; Kass et al. 2003). The response latency (T) was defined as the time gap between the stimulus onset and the peak response. The maximum level (R) of the curve was taken as the peak firing rate of the response. The response duration (D) was defined as the time over which response falls from R to R/e (Fig. 1a). For the dual-peak response, these parameters were calculated for each peak respectively (T_1, R_1, D_1 for the first peak; T_2, R_2, D_2 for the second peak).

Statistical analysis

Statistics were performed using Matlab (version 7.0.0, The MathWorks, Inc., Natick, MA, USA). Results were presented as mean ± SEM. Student's *t*-test was used to determine the statistical significance between two groups, and one-way analysis of variance (ANOVA) was used for comparison among multiple groups (>2), with $p < 0.05$ indicating significant difference. If a significant p value was obtained for ANOVA, post hoc analysis was performed using Student–Newman–Keuls (SNK) test. Regarding the analysis of the bimodality in the distribution of response latency, Hartigan's dip test was used (Hartigan and Hartigan 1985).

Results

Dual-peak responses in mouse RGC

In exposure to periodic 1s-ON/1s-OFF full-field white light flashes, mouse RGCs show various response patterns: sustained ON response, transient ON response, sustained OFF response, transient OFF response and ON–OFF response, which were in accordance with previously reported observations (Nirenberg and Meister 1997; Farrow and Masland 2011). In addition, it was also observed that in some ON- or ON–OFF RGCs, the ON response exhibited two peaks in the PSTH, which was referred to as dual-peak response. Typically, this dual-peak response was composed of a transient component and another following component occurring shortly after the initial one. In our experiments, the dual-peak responses recorded were mostly ON responses, so we focused our analysis on the light-ON part of the responses recorded. In our experiments, 49 RGCs presenting dual-peak responses from 10 retinas were recorded.

To quantitatively describe the temporal properties of the dual-peak responses, three parameters were measured: response latency, peak firing rate and response duration for the two peaks respectively (see "Materials and methods").

For the example neuron presented in Fig. 1a, the first response peak had a short latency ($T_1 = 120.0$ ms), a high peak firing rate ($R_1 = 69.5$ Hz) and a short duration ($D_1 = 20.0$ ms), while the second peak showed a longer latency ($T_2 = 245.0$ ms), a relatively lower peak firing rate ($R_2 = 35.7$ Hz), and a short duration ($D_2 = 30.0$ ms). For another example neuron presented in Fig. 1b, the first and second peak respectively exhibited characteristics similar to that of the neuron in Fig. 1a ($T_1 = 115.0$ ms, $R_1 = 87.6$ Hz, $D_1 = 25.0$ ms, $T_2 = 230.0$ ms, $R_2 = 44.0$ Hz), except for a long duration of the second peak ($D_2 = 330.0$ ms).

Statistical results from RGCs (N = 49 from 10 retinas) presenting dual-peak response patterns also showed that the two peaks exhibited distinct temporal dynamics. The first peak was with a short latency ($T_1 = 124.5 \pm 2.1$ ms) and a high peak firing rate ($R_1 = 74.7 \pm 6.6$ Hz). It was always with a short duration that generally lasted for less than 50 ms ($D_1 = 21.8 \pm 1.4$ ms). In contrast, the second peak was quite sluggish, with a longer latency ($T_2 = 245.0 \pm 5.9$ ms) and a lower peak firing rate ($R_2 = 40.7 \pm 2.8$ Hz). Besides, the duration of the second peak was widely distributed, over a range of 10–345 ms. The large variation in the duration of the second peak suggests that the neural circuitry related to the second peak should be more complicated and diversified than that of the first peak.

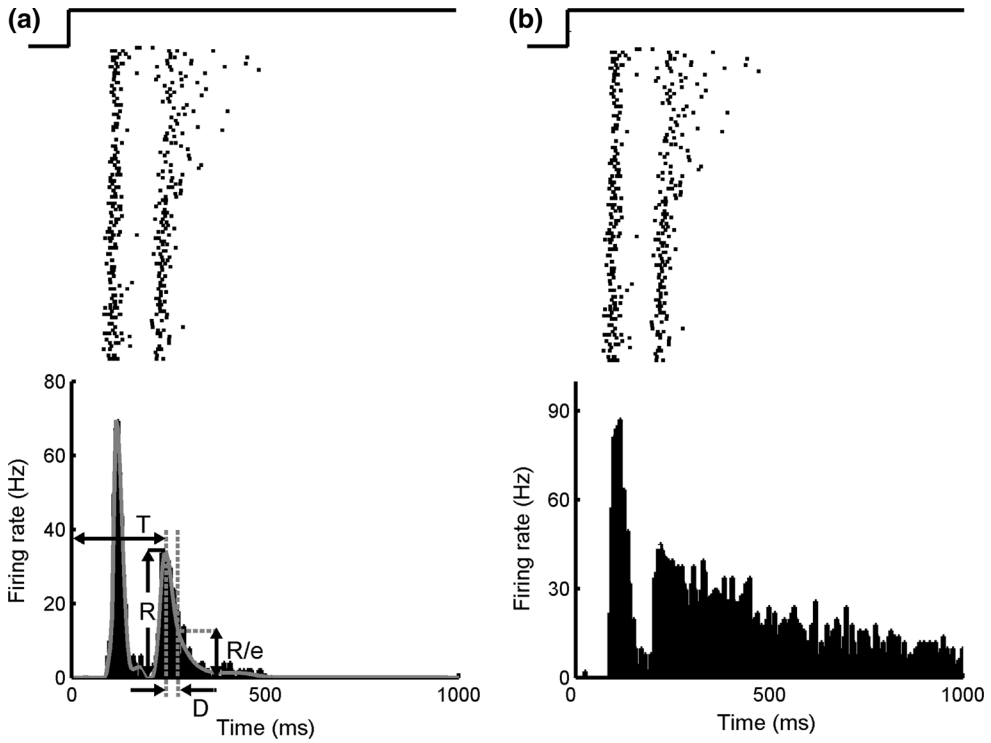

Fig. 1 Different temporal patterns shown in the second peak of the dual-peak responses. **a** *Raster plot* (*top panel*) and PSTH (*bottom panel*, bin size = 5 ms) of an RGC with the dual-peak response, in which the second peak had a short duration (30.0 ms). Definitions of latency (T), peak firing rate (R) and duration (D) of response are shown. **b** *Raster plot* (*top panel*) and PSTH (*bottom panel*, bin size = 5 ms) of another RGC with the dual-peak response, in which the second peak had a long duration (330.0 ms). The traces above the *raster plots* in (**a**, **b**) illustrate the onset and duration of the light stimulation (1 s)

Similarity in temporal properties of the dual-peak responses and single-peak responses

Apart from the dual-peak responses, single-peak ON responses with different latencies were also observed. Figure 2a shows an example neuron with a short response latency of 115.0 ms while Fig. 2b shows another neuron with a long response latency of 240.0 ms. Figure 2c illustrates the distribution of response latencies obtained from 94 single-peak ON cells of 10 retinas. According to Hartigan's dip test (Hartigan and Hartigan 1985; Kastner and Baccus 2011), the distribution was significantly bimodal ($p < 0.05$). The black curve in Fig. 2c illustrates the probability density function fitted by kernel density estimate (Rosenblatt 1956; Parzen 1962; Fisher and Marron 2001). The probability density function had a valley being around 170 ms (indicated by a dashed line in Fig. 2c). Single-peak ON responses were thus categorized into two groups, with "short-latency response" defined as that with a latency shorter than 170 ms, and "long-latency response" defined as that with a latency longer than 170 ms. Following this criterion, among the total amount of 94 RGCs with single-peak ON responses, 61 belonged to the short-latency group and the remaining 33 belonged to the long-latency group. The comparison between the single-peak responses and the dual-peak responses showed that the temporal properties of the short- and long-latency responses were similar to those of the first peak and the second peak of the dual-peak responses, respectively.

In our experiments, a total number of 143 RGCs, including 49 with dual-peak responses, 61 with short-latency single-peak responses and 33 with long-latency single-peak responses were recorded from 10 retinas, and the comparison of the temporal properties was performed among these cells. As shown in Fig. 2d, the average latency for the first peak of the dual-peak response was very similar to that of the short-latency response (124.5 ± 2.1 ms and 120.2 ± 2.4 ms, respectively), while the latency of the second peak was quite similar to that of the long-latency response (245.0 ± 5.9 ms and 247.4 ± 8.1 ms, respectively). Meanwhile, the latencies of the first peak and the short-latency response were significantly shorter as compared to that of the second peak and the long-latency response (ANOVA, $p < 0.01$). The peak firing rates of different response patterns were also compared (Fig. 2e). The results showed that there was no significant difference between the first peak (74.7 ± 6.6 Hz) and the short-latency response (71.8 ± 5.8 Hz), or between the

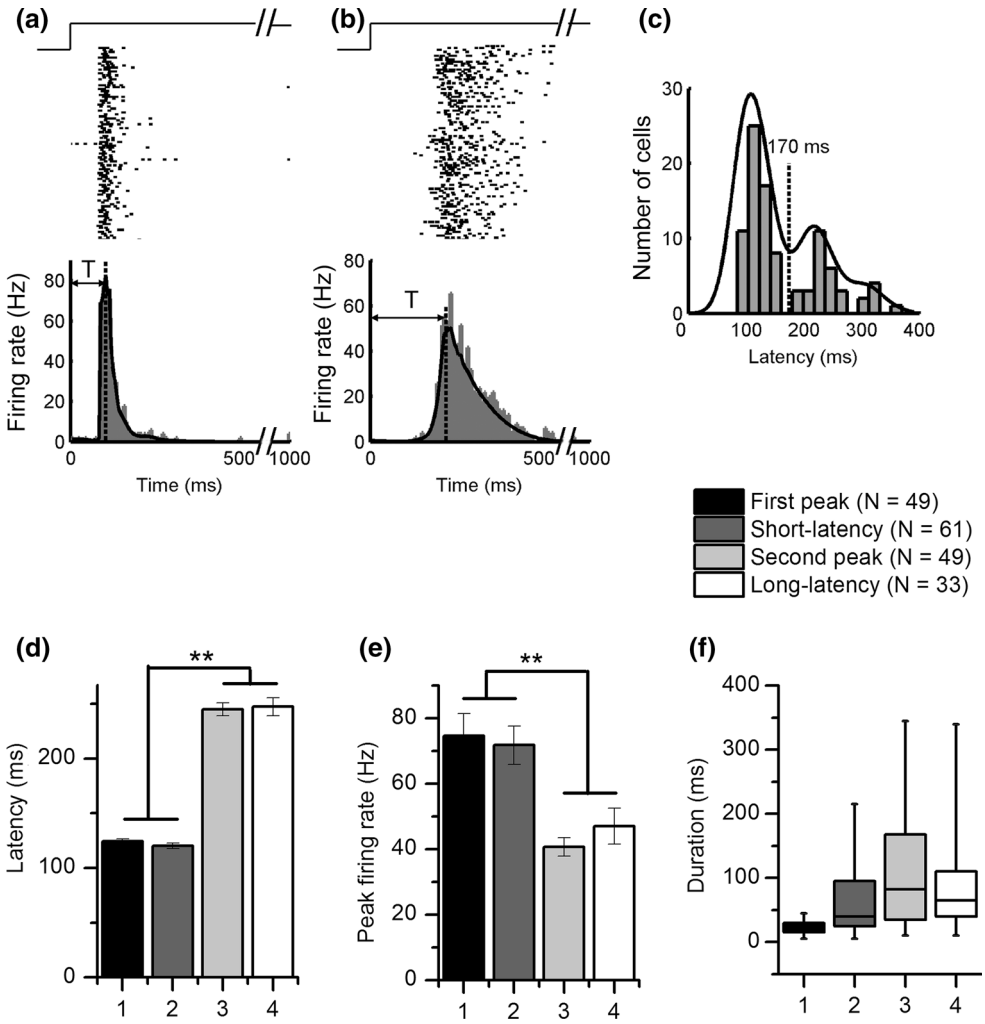

Fig. 2 The comparison of the temporal properties between the dual-peak responses and the single-peak responses. **a** *Raster plot* (*top panel*) and PSTH (*bottom panel*, *gray bar*, bin size = 5 ms) of an RGC with a short latency (T = 115.0 ms). **b** *Raster plot* (*top panel*) and PSTH (*bottom panel*, *gray bar*, bin size = 5 ms) of another RGC with a long latency (T = 240.0 ms). The traces above the *raster plots* in (**a**, **b**) illustrate the onset and duration of the light stimulation (1 s). **c** Distribution of response latencies for single-peak ON responses (N = 94), which was significantly bimodal (Hartigan's dip test, $p < 0.05$). The two groups are separated by a *vertical dash line* (latency = 170 ms). **d** *Bar plots* showing mean response latencies (mean ± SEM, **, $p < 0.01$, ANOVA). **e** *Bar plots* showing mean peak firing rates (mean ± SEM, **, $p < 0.01$, ANOVA). **f** *Box-plots* of the distributions of the durations for different response patterns. *Horizontal box lines* represent the 25th quartile, median and 75th quartile value of the distribution, respectively. The end of the *vertical line* extends from the *top* and the *bottom* of the *box* indicates the maximum value and minimum value, respectively

second peak (40.7 ± 2.8 Hz) and the long-latency response (47.0 ± 5.5 Hz). Moreover, the peak firing rates of the first peak and the short-latency response were significantly higher as compared to that of the second peak and the long-latency response (ANOVA, $p < 0.01$). The distributions of response durations for each of the four groups are illustrated in Fig. 2f. For the dual-peak response, the duration of the first peak was short and distributed within a limited range, whereas that of the second peak varied greatly from tens to hundreds of milliseconds, which resembled that of the single-peak response.

These results show that the first peak of the dual-peak response exhibited similar temporal properties as the short-latency transient response, and the temporal properties of the second peak resembled those of the long-latency response.

Effects of the inhibitory pathway(s) on the dual-peak responses

GABA and glycine are both important inhibitory neurotransmitters in retinas and have been demonstrated to play important roles in modulating retinal neurons' activities (Yang 2004; Shen and Jiang 2007). To study possible effects of inhibitory pathway(s) on dual-peak responses,

exogenous GABA (250 μM) and glycine (100 μM) were applied.

In one set of our experiments, GABA was applied first, and then glycine was added in the continuous presence of GABA. Figure 3a shows the response of an example RGC with the dual-peak pattern in normal Ringer's solution. When GABA was applied to the retina, there was a modest reduction in the peak firing rate of the first peak (88.9 Hz in control, 77.7 Hz in GABA), while the second peak was completely eliminated (Fig. 3b). Additional application of glycine led to further decrease in peak firing rate for the first peak (69.1 Hz in GABA + glycine, Fig. 3c). Figure 3d–f show the responses of another RGC with the dual-peak pattern during control, GABA application and co-application of GABA + glycine. The result showed that GABA application slightly decreased the firing rate of the first peak (73.3 Hz in control, 61.0 Hz in GABA), while the second response peak was largely suppressed (27.8 Hz in control, 11.0 Hz in GABA, Fig. 3e). Additional application of glycine led to further decrease in peak firing rate for the first peak (56.8 Hz in GABA + glycine) and complete elimination of the second peak (Fig. 3f). The second response peak recovered after 1 h of washout (data not shown).

Statistical results of 16 neurons presenting the dual-peak responses from 7 retinas showed that during GABA application, the first peak was largely maintained with a modest reduction in the peak firing rate (Fig. 3g, paired t test, $p < 0.05$). Whereas in 9 neurons, the second peak was completely eliminated, and in the remaining 7 neurons, it was greatly suppressed (Fig. 3h, paired t test, $p < 0.05$). Additional application of glycine in the continuous presence of GABA resulted in further decrease in the peak firing rate of the first peak (Fig. 3i, paired t test, $p < 0.05$), while it completely eliminated the second peak.

To further confirm the inhibitory effects of GABA and glycine, we altered the order of drug application: glycine was applied first, and then GABA in the continuous presence of glycine. As an example, for the neuron presented in Fig. 4a–c, glycine application suppressed the firing activities in the first peak of the dual-peak response (82.2 Hz in control, 65.9 Hz in glycine), while the second peak was completely eliminated (Fig. 4b). Additional application of GABA led to further decrease in the peak firing rate of the first peak (56.8 Hz in co-application of glycine + GABA, Fig. 4c). Figure 4d–f show the responses of another RGC with the dual-peak pattern. Glycine application decreased the firing rate of the first peak (84.3 Hz in control, 70.0 Hz in glycine) and greatly suppressed that of the second peak (50.9 Hz in control, 21.4 Hz in glycine, Fig. 4e). Additional application of GABA led to further decrease in the peak firing rate of the first peak (61.8 Hz in co-application of glycine + GABA), and completely eliminated the second peak (Fig. 4f). The second response peak recovered after 1 h of washout (data not shown).

Statistical results of 17 neurons with the dual-peak responses from 6 retinas showed that during glycine application, the first peak was largely maintained, with a modest reduction in the peak firing rate (Fig. 4g, paired t test, $p < 0.05$). Among these, the second peak was completely eliminated in 9 neurons, and it was greatly suppressed in the remaining 8 neurons (Fig. 4h, paired t test, $p < 0.05$). Additional application of GABA in the continuous presence of glycine resulted in further decrease in the peak firing rate of the first peak (Fig. 4i, paired t test, $p < 0.05$), while it completely eliminated the second peak.

Picrotoxin (PTX) and strychnine are the antagonists of GABA and glycine receptors, respectively. In further experiments, PTX (40 μM) and strychnine (5 μM) were added to confirm the effects of GABAergic and glycinergic pathways on the dual-peak responses of mouse RGCs.

The effect of PTX on dual-peak responses is shown in Fig. 5a, b. The example neuron exhibited the dual-peak pattern in normal Ringer's solution (Fig. 5a). When PTX was applied to the retina, the response pattern was remained (Fig. 5b). Statistical results showed that 14 RGCs (100 %) from 5 retinas with dual-peak patterns in control exhibited the same response pattern when PTX was added.

Similar to PTX, application of strychnine also did not block the dual-peak response. Figure 5c, d show the responses of another ganglion cell in control and in strychnine, respectively. The dual-peak pattern was observed in both control condition and during strychnine application. Such phenomenon was observed in 13 RGCs (100 %) from 5 retinas.

These results revealed that blockade of GABAergic and glycinergic pathways were ineffective in transforming the dual-peak pattern into single-peak pattern with sustained activities.

Besides, it was found that the dual-peak responses could be induced in some RGCs with transient single-peak responses, with a second response phase being unmasked in the presence of PTX and/or strychnine. Figure 6a, b give an example in which the tested neuron showed transient response in normal Ringer's solution. When PTX was applied to the retina, a second response phase was elicited, with a latency of 290.0 ms, a peak firing rate of 50.3 Hz, and a duration of 25.0 ms. In the meantime, the response properties of the first peak changed slightly ($T_1 = 120.0$ ms, $R_1 = 89.5$ Hz, $D_1 = 20.0$ ms in control; $T_1 = 125.0$ ms, $R_1 = 98.1$ Hz, $D_1 = 20.0$ ms in PTX). On washing out of PTX, transient response can be observed again (data not shown).

Statistical results showed that when PTX was added, 13 out of 20 RGCs with transient responses from 5 retinas exhibited an unmasked second response peak, which had a

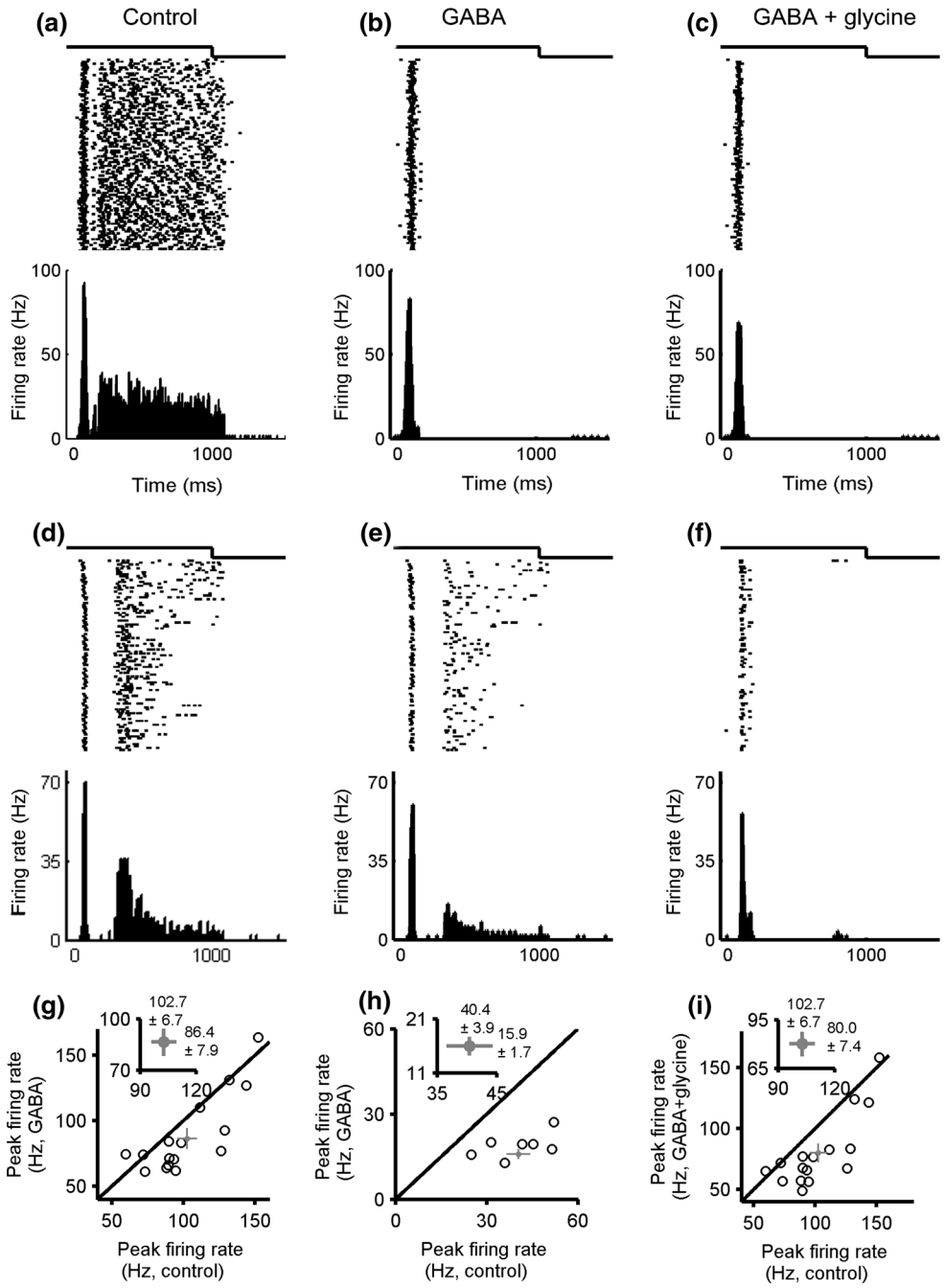

Fig. 3 The effect of exogenous GABA (250 μM) and additive glycine (100 μM, in the continuous presence of GABA) on the dual-peak responses. **a** *Raster plot* (*top panel*) and PSTH (*bottom panel*, bin size = 5 ms) from an RGC exhibiting the dual-peak pattern in control. **b** *Raster plot* and PSTH from the RGC (same as shown in **a**) of which the second peak was eliminated during GABA application. **c** *Raster plot* and PSTH from the RGC (same as shown in **a**) during co-application of GABA + glycine. **d** *Raster plot* and PSTH of another RGC exhibiting the dual-peak pattern in control. **e** *Raster plot* and PSTH from the RGC (same as shown in **d**) of which the firing activities in the second peak were greatly suppressed during GABA application. **f** *Raster plot* and PSTH from the RGC (same as shown in **d**) of which the second peak was completely eliminated with additional application of glycine (in the continuous presence of GABA). The traces above the *raster plots* in (**a**–**f**) illustrate the time course of the light stimulation. **g** *Scatter plot* of the peak firing rate for the first peak during control (abscissa) and GABA (ordinate) (N = 16 neurons from 7 retinas). **h** *Scatter plot* of the peak firing rate for the second peak during control (abscissa) and GABA (ordinate) (N = 7 neurons from 7 retinas). **i** *Scatter plot* of the peak firing rate for the first peak during control (abscissa) and co-application of GABA + -glycine (ordinate) (N = 16 neurons from 7 retinas). The *gray crosses* in (**g**–**i**) indicate mean ± SEM, which are magnified in the *inset* on the *top left*. The *diagonal lines* in (**g**–**i**) represent equality

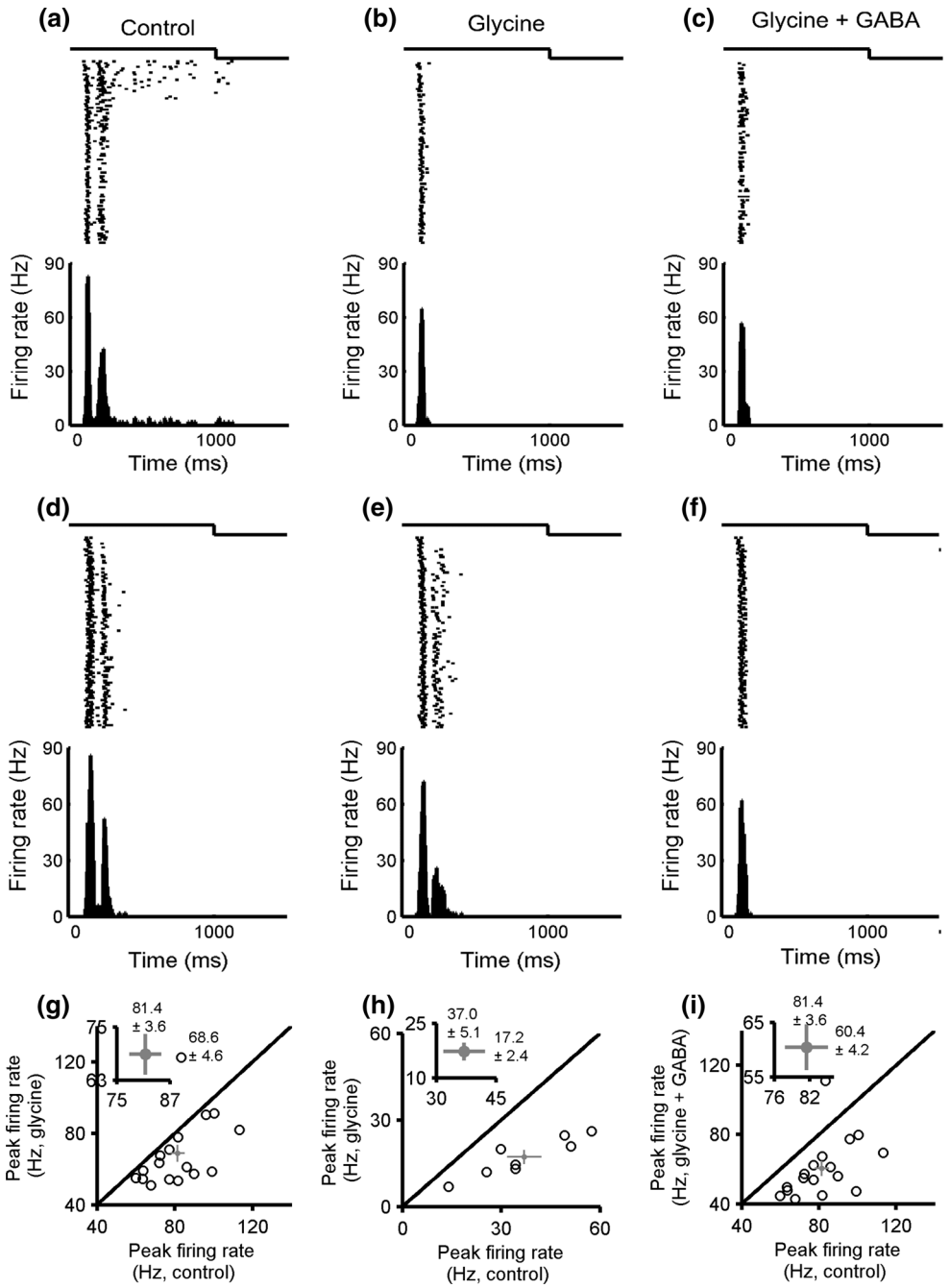

Fig. 4 The effect of exogenous glycine (100 μM) and additive GABA (250 μM, in the continuous presence of glycine) on the dual-peak responses. **a** *Raster plot* (*top panel*) and PSTH (*bottom panel*, bin size = 5 ms) from an RGC exhibiting the dual-peak pattern in control. **b** *Raster plot* and PSTH from the RGC (same as shown in **a**) of which the second peak was eliminated during glycine application. **c** *Raster plot* and PSTH from the RGC (same as shown in **a**) during co-application of glycine + GABA. **d** *Raster plot* and PSTH of another RGC exhibiting the dual-peak pattern in control. **e** *Raster plot* and PSTH from the RGC (same as shown in **d**) of which the firing activities in the second peak were greatly suppressed during glycine application. **f** *Raster plot* and PSTH from the RGC (same as shown in **d**) of which the second peak was eliminated with additional application of GABA (in the continuous presence of glycine). The traces above the *raster plots* in (**a**–**f**) illustrate the time course of the light stimulation. **g** *Scatter plot* of the peak firing rate for the first peak during control (abscissa) and glycine (ordinate) (N = 17 neurons from 6 retinas). **h** *Scatter plot* of the peak firing rate for the second peak during control (abscissa) and glycine (ordinate) (N = 8 neurons from 6 retinas). **i** *Scatter plot* of the peak firing rate for the first peak during control (abscissa) and co-application of glycine + GABA (ordinate) (N = 17 neurons from 6 retinas). The *gray crosses* in (**g**–**i**) indicate mean ± SEM, which are magnified in the *inset* on the *top left*. The *diagonal lines* in (**g**–**i**) represent equality

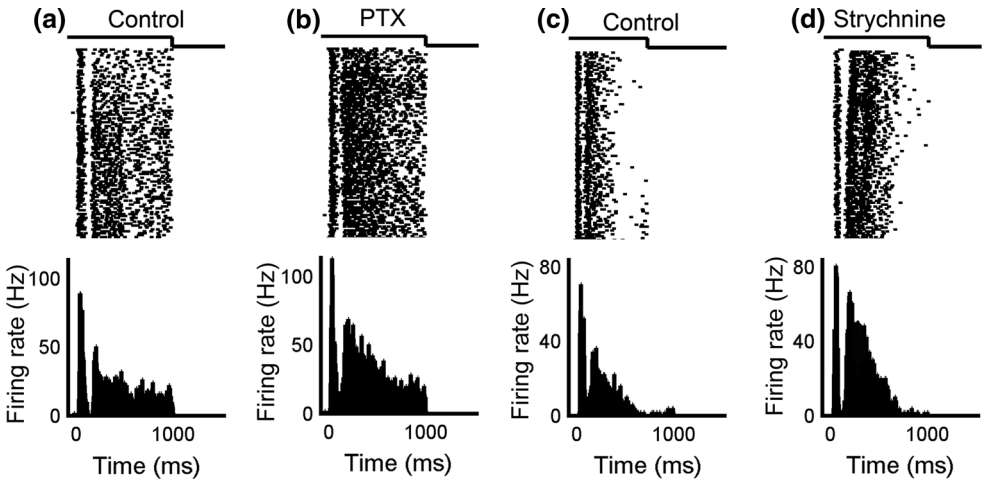

Fig. 5 The effect of PTX (40 μM) and strychnine (5 μM) on the dual-peak responses. **a**, **b** *Raster plots* (*top panels*) and PSTHs (*bottom panels*, bin size = 5 ms) of an RGC exhibiting the dual-peak pattern in control and during PTX application, respectively. **c**, **d** *Raster plots* and PSTHs of another RGC exhibiting the dual-peak pattern in control and during strychnine application, respectively. The traces above the *raster plots* in (**a**–**d**) illustrate the time course of the light stimulation

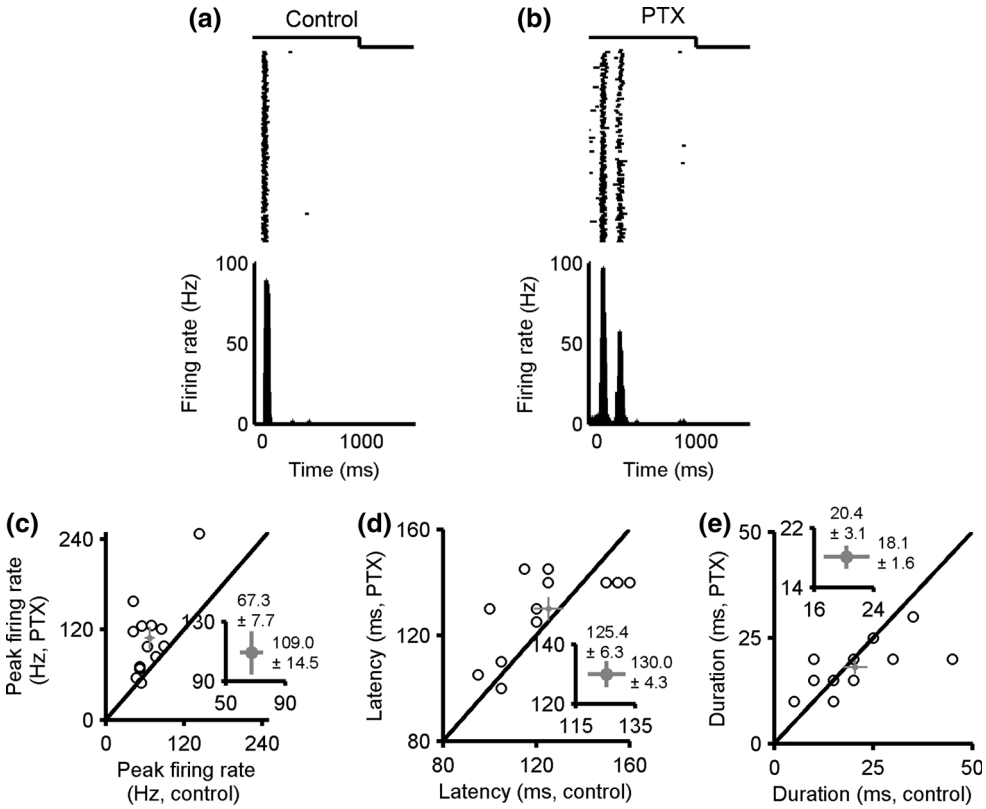

Fig. 6 The induction of the dual-peak responses in some transient RGCs by PTX (40 μM). **a** *Raster plot* (*top panel*) and PSTH (*bottom panel*, bin size = 5 ms) from an RGC with transient response in control. **b** *Raster plot* and PSTH from the RGC (same as shown in **a**) during PTX application show that PTX could unmask a second response peak. The traces above the *raster plots* in (**a**, **b**) illustrate the time course of the light stimulation. **c** *Scatter plot* of the peak firing rate for the first peak during control (abscissa) and PTX (ordinate) (N = 13 neurons from 5 retinas). **d** *Scatter plot* of the latency for the first peak during control (abscissa) and PTX (ordinate). **e** *Scatter plot* of the duration for the first peak during control (abscissa) and PTX (ordinate). The *gray crosses* in (**c**–**e**) indicate mean ± SEM, which are magnified in the *inset*. The *diagonal lines* in (**c**–**e**) represent equality

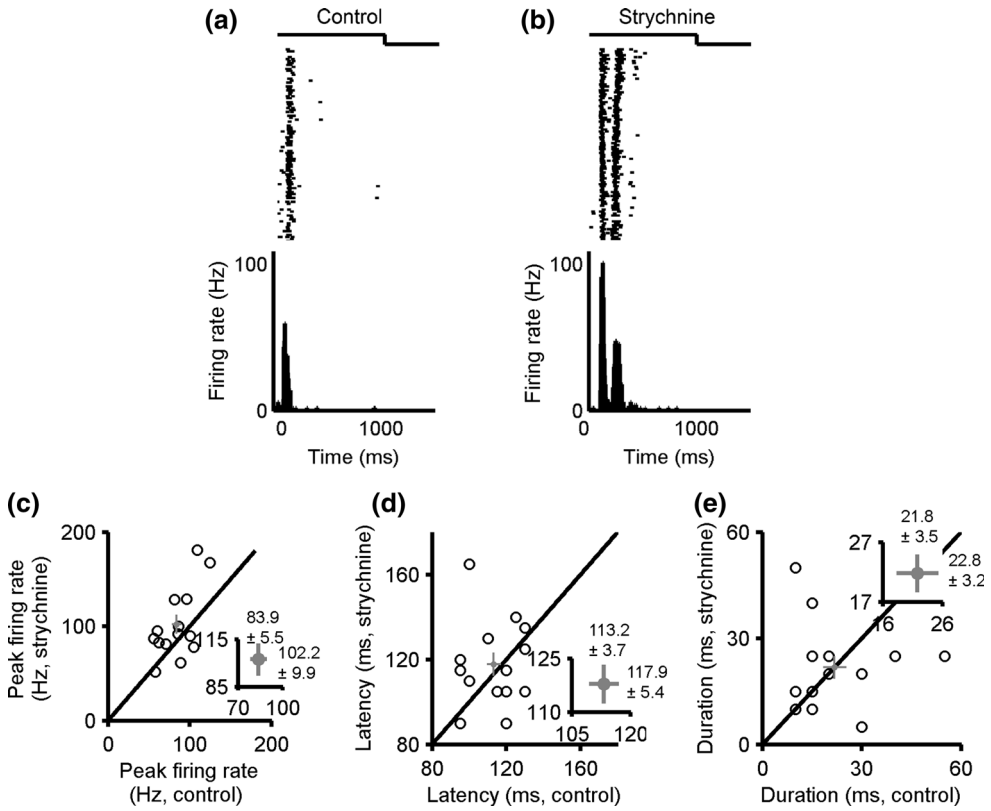

Fig. 7 The induction of the dual-peak responses in some transient ganglion cells by strychnine application (5 μM). **a** *Raster plot* (*top panel*) and PSTH (bottom panel, bin size = 5 ms) from an RGC with transient response in control. **b** *Raster plot* and PSTH from the RGC (same as shown in **a**) during strychnine application show that strychnine could unmask a second response peak. The traces above the *raster plots* in (**a**–**b**) illustrate the time course of the light stimulation. **c** *Scatter plot* of the peak firing rate for the first peak during control (abscissa) and strychnine (ordinate) (N = 14 neurons from 5 retinas). **d** *Scatter plot* of the latency for the first peak during control (abscissa) and strychnine (ordinate). **e** *Scatter plot* of the duration for the first peak during control (abscissa) and strychnine (ordinate). The *gray crosses* in (**c**–**e**) indicate mean ± SEM, which are magnified in the *inset*. The *diagonal lines* in (**c**–**e**) represent equality

long latency ($T_2 = 293.1 \pm 12.8$ ms), a low peak firing rate ($R_2 = 37.4 \pm 4.0$ Hz) and a duration (D_2) distributed between 10 and 80 ms. Meanwhile, for the first peak, the peak firing rate was significantly increased with PTX application (Fig. 6c, paired *t* test, $p < 0.05$), while both the latency (Fig. 6d, paired *t* test, $p > 0.05$) and duration (Fig. 6e, paired *t* test, $p > 0.05$) exhibited no significant changes. This result was consistent with the result that the second peak of the dual-peak response was eliminated or largely suppressed during GABA perfusion.

Strychnine had an effect similar to that of PTX, inducing the dual-peak responses in some RGCs with transient responses. As the example plotted in Fig. 7a, b, the RGC showed transient response in normal Ringer's solution (Fig. 7a). When strychnine was applied to the retina, a second response phase was elicited, with a latency of 260.0 ms, a peak firing rate of 48.4 Hz and duration of 35.0 ms (Fig. 7b). In the meantime, some changes in the response properties of the first peak were observed ($T_1 = 115.0$ ms, $R_1 = 60.3$ Hz, $D_1 = 20.0$ ms in control; $T_1 = 120.0$ ms, $R_1 = 95.4$ Hz, $D_1 = 20.0$ ms in strychnine). After washout of strychnine, the induced second peak disappeared, and transient response recovered (data not shown).

Among the 33 cells with transient responses from 5 retinas, 14 showed such changes. The induced second peak had a long latency ($T_2 = 277.1 \pm 9.6$ ms), a low peak firing rate ($R_2 = 32.4 \pm 4.4$ Hz) and a duration (D_2) distributed between 20 and 390 ms. Meanwhile, the application of strychnine resulted in an increase of the peak firing rate for the first peak (Fig. 7c, paired *t* test, $p < 0.05$), but had no significant effect on latency (Fig. 7d, paired *t* test, $p > 0.05$) and duration (Fig. 7e, paired *t* test, $p > 0.05$).

Putting together, these results indicate that both GABAergic and glycinergic pathways are involved in mediating the properties of the dual-peak responses of the mouse RGCs.

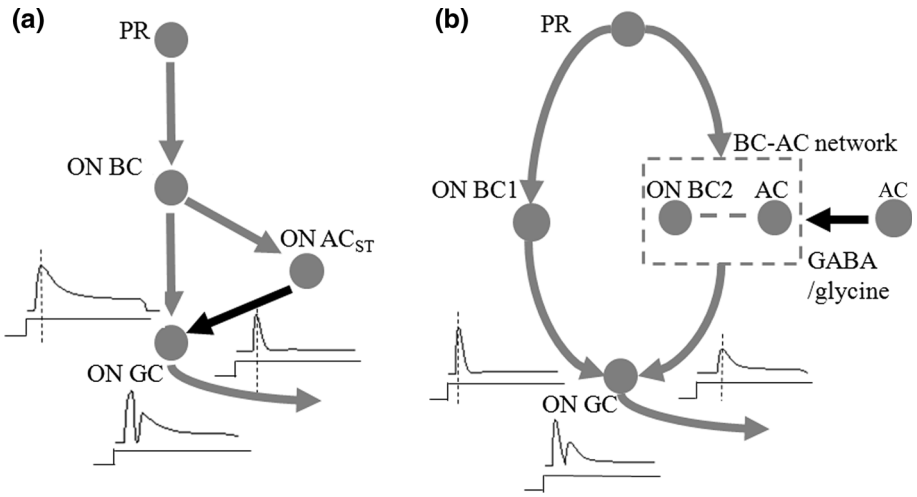

Fig. 8 Two possible neural circuits which may underlie the generation of the dual-peak response. **a** Schematic illustration of the neural circuit in which an inhibitory signal generated by amacrine cell is superimposed on a sustained excitatory signal generated by bipolar cell to produce the dual-peak response. *PR* photoreceptor, *ON BC* ON-center bipolar cell, *ON* AC_{ST} ON-center sluggish transient amacrine cell, the existence of which was previously reported (Marchiafava and Weiler 1982; Werblin 2011); *ON-GC* ON-center ganglion cell. The responses of the ON BC, ON AC_{ST} and ON GC are respectively plotted, with traces below illustrating the onset of the light stimulation and the *dotted vertical lines* marking the peak response. *Gray arrows* indicate sign conserving connections, while *black arrow* indicates sign inverting connection. **b** Schematic illustration of the neural circuit in which excitatory signals generated by two pathways with different latencies converge on the RGC. *PR* photoreceptor, *ON BC* ON-center bipolar cell, *AC* amacrine cell, *ON-GC* ON-center ganglion cell. The pathway related to the second response peak might involve a more complex amacrine cell network, and could be masked by the inhibitory inputs and induced when the inhibitory signals are weakened. The responses of the two pathways are plotted, with traces below illustrating the onset of the light stimulation and the *dotted vertical lines* marking the peak response. *Gray arrows* indicate sign conserving connections, while *black arrow* indicates sign inverting connections

Discussion

In the present study, we investigated the temporal properties of the dual-peak responses recorded in mouse RGCs elicited by spatially homogeneous light flashes and the effect of the inhibitory input mediated by GABAergic and/or glycinergic pathways. The two peaks of the dual-peak responses exhibited distinct temporal dynamics. The first peak occurred rapidly at the stimulus onset with a relatively high firing rate and a short duration, exhibiting properties similar to those of the short-latency single-peak transient response. In contrast, the second peak could be either transient or sustained, with a long latency and a low peak firing rate, showing temporal properties similar to those of long-latency single-peak response. Pharmacological studies demonstrated that when GABA or glycine was applied, the second response peak could be suppressed or even eliminated, while little change was induced in the first peak. Moreover, blockade of GABAergic or glycinergic pathway(s) could induce the dual-peak responses in some transient cells by unmasking a second response phase.

Effect of GABAergic and glycinergic pathways on dual-peak responses

It was previously proposed that dual-peak response was generated by an inhibitory process which suppressed the ganglion cell's activity, with the duration of the inhibitory signal from amacrine cells shorter than that of the excitatory signal from bipolar cells, this resulting in two peaks in the cell's responsiveness (Thiel et al. 2006) (Fig. 8a). If this was the case, application of inhibitory receptor antagonists should have resulted in the transformation from the dual-peak pattern to single-peak pattern with sustained activities. However, our experiments revealed blockade of GABA and glycine receptors, either alone or in combination, was ineffective at this transformation (Fig. 5). Thus, the dual-peak response of mouse RGCs observed in our experiments is not likely to be attributed to an inhibitory input superimposed on a sustained excitatory input.

On the other hand, the present study demonstrated that blockade of GABAergic or glycinergic pathway could cause a late component in some ganglion cells with transient response patterns and thus induce the dual-peak responses (Figs. 6, 7). Similar effect has been previously observed in mouse and non-mammalian retinas with PTX application (Nirenberg and Meister 1997; Dong and Werblin 1998; Popova et al. 2003). Besides, we also tested the role of GABA and glycine, and found that both drugs could largely suppress or even eliminate the second peak in the dual-peak responses. These results confirm the important roles that GABAergic and glycinergic pathways play in the mediating the dual-peak responses. This also indicates that the two response peaks may originate from distinct

pathways, with the pathway related to the second response peak being masked by the inhibitory inputs and being induced when the inhibitory signals are weakened.

The origin of the two response peaks in the dual-peak responses

It was found in the present study that among mouse RGCs, there are certain similarities in temporal properties and pharmacological properties (data not shown) between the first peak of the dual-peak response and short-latency response, and between the second peak and long-latency response, respectively (Fig. 2). In our present study, the short- and long-latency RGCs were classified on the basis of the bimodal latency distribution of the cells' responses to full-field white light flashes, with the former and latter being respectively classified as those with latencies shorter and longer than 170 ms (Fig. 2c).

In other mammalian retinas, ganglion cells with short and long latencies have also been reported and classified as brisk and sluggish cells (van Wyk et al. 2006; Heine and Passaglia 2011). In rat retina, the brisk cells had a mean latency (defined as the time lag between the stimulus onset and the peak response, as adopted in the present study) around 70 ms, while sluggish cells had a mean latency around 180 ms (Heine and Passaglia 2011). Such response parameter distributions were similar to those observed in our present study. In rabbit retina, RGCs can also be classified into brisk and sluggish subtypes based on their response latencies: time to half-peak response was about 200 and 500 ms for brisk and sluggish cells respectively (van Wyk et al. 2006; Venkataramani et al. 2014). The differences in response latency distributions between observation made from rodent and rabbit retinas may be attributed to species-related differences.

Regarding the origin of the brisk and sluggish responses in ganglion cells, synaptic-based studies suggested that the temporal properties of the two responses were partly resulted from the different kinetics of the presynaptic excitatory inputs—the kinetics of excitatory bipolar inputs for brisk cells was faster than that for sluggish cells (van Wyk et al. 2006; Buldyrev and Taylor 2013). Another factor may be the different inhibitory microcircuits involved in the neural circuitry. For brisk cells, the excitatory signal had a faster kinetics compared with the inhibitory signal, while for sluggish cells, it was exactly the opposite that the inhibitory signal even had a faster kinetics than the excitatory signal. This inhibitory signal was hence effective to suppress early spiking activities, which was consistent with the sluggish activities of the cells (van Wyk et al. 2006; Buldyrev and Taylor 2013). Besides, the strengths of the inhibitory inputs eventually affect the firing rates of the ganglion cell responses, which lead to the different firing rates for the short- and long-latency pathways. Therefore, it is reasonable to speculate that in the present study, the different properties of short- and long-latency responses may result from different bipolar cell inputs and different inhibitory circuits involved.

Considering the similarities in the temporal properties and pharmacological properties between the dual-peak response and short- and long-latency responses, the generation of the dual-peak response might originate from the convergence of the two pathways related to the short-latency response and long-latency response. However, blockaded of inhibitory signal pathway(s) had little effect on the dual-peak response. Thus the differences in the two peaks are likely due to the different kinetics of the presynaptic excitatory inputs, which are probably related to the different properties of bipolar cells in the circuits. Besides, the second peak might be generated by a more complex amacrine cell network (Fig. 8b), which may include the "serial inhibitory" connections (Zhang et al. 1997; Roska et al. 1998; Eggers and Lukasiewicz 2010).

Acknowledgments This work was supported by Grants from National Foundation of Natural Science of China (No. 31471054, P.J.L; No. 61375114, P.M.Z).

Compliance with ethical standards

The experimental procedures described in the study involving animal experiments were reviewed and approved by Institutional Animal Care and Use Committee at Shanghai Jiao Tong University.

Conflict of interest The authors declare that they have no conflict of interest.

References

Awatramani GB, Slaughter MM (2000) Origin of transient and sustained responses in ganglion cells of the retina. J Neurosci 20(18):7087–7095

Buldyrev I, Taylor WR (2013) Inhibitory mechanisms that generate centre and surround properties in ON and OFF brisk-sustained ganglion cells in the rabbit retina. J Physiol 591(1):303–325. doi:10.1113/jphysiol.2012.243113

Carcieri SM, Jacobs AL, Nirenberg S (2003) Classification of retinal ganglion cells: a statistical approach. J Neurophysiol 90(3):1704–1713. doi:10.1152/jn.00127.2003

Cleland BG, Levick WR (1974) Brisk and sluggish concentrically organized ganglion cells in the cat's retina. J Physiol 240(2):421–456

Dimatteo I, Genovese CR, Kass RE (2001) Bayesian curve-fitting with free-knot splines. Biometrika 88(4):1055–1071

Dong C-J, Werblin FS (1998) Temporal contrast enhancement via $GABA_C$ feedback at bipolar terminals in the tiger salamander retina. J Neurophysiol 79(4):2171–2180

Eggers ED, Lukasiewicz PD (2010) Interneuron circuits tune inhibition in retinal bipolar cells. J Neurophysiol 103(1):25–37

Farrow K, Masland RH (2011) Physiological clustering of visual channels in the mouse retina. J Neurophysiol 105(4):1516–1530. doi:10.1152/jn.00331.2010

Fisher NI, Marron JS (2001) Mode testing via the excess mass estimate. Biometrika 88(2):499–517

Greschner M, Thiel A, Kretzberg J, Ammermüller J (2006) Complex spike-event pattern of transient ON–OFF retinal ganglion cells. J Neurophysiol 96(6):2845–2856. doi:10.1152/jn.01131.2005

Hamasaki DI, Winters RW (1974) A review of the properties of sustained and transient retinal ganglion cells. Experientia 30(7):713–719

Hartigan JA, Hartigan PM (1985) The dip test of unimodality. Ann Stat 13(1):70–84

Heine WF, Passaglia CL (2011) Spatial receptive field properties of rat retinal ganglion cells. Vis Neurosci 28(5):403–417. doi:10.1017/S0952523811000307

Ishii T, Kaneda M (2014) ON-pathway-dominant glycinergic regulation of cholinergic amacrine cells in the mouse retina. J Physiol 592(19):4235–4245

Jing W, Liu W-Z, Gong X-W, Gong H-Q, Liang P-J (2010a) Visual pattern recognition based on spatio-temporal patterns of retinal ganglion cells' activities. Cogn Neurodyn 4(3):179–188. doi:10.1007/s11571-010-9119-8

Jing W, Liu W-Z, Gong X-W, Gong H-Q, Liang P-J (2010b) Influence of GABAergic inhibition on concerted activity between the ganglion cells. NeuroReport 21(12):797–801. doi:10.1097/WNR.0b013e32833c5b50

Kass RE, Ventura V, Cai C (2003) Statistical smoothing of neuronal data. Netw: Comput Neural Syst 14(1):5–15

Kastner DB, Baccus SA (2011) Coordinated dynamic encoding in the retina using opposing forms of plasticity. Nat Neurosci 14(10):1317–1322. doi:10.1038/nn.2906

Liu X, Zhou Y, Gong H-Q, Liang P-J (2007) Contribution of the GABAergic pathway(s) to the correlated activities of chicken retinal ganglion cells. Brain Res 1177:37–46. doi:10.1016/j.brainres.2007.07.001

Marchiafava PL, Weiler R (1982) The photoresponses of structurally identified amacrine cells in the turtle retina. Proc R Soc Lond B Biol Sci 214(1196):403–415

Masland RH (2001) The fundamental plan of the retina. Nat Neurosci 4(9):877–886. doi:10.1038/nn0901-877

McCall MA, Lukasiewicz PD, Gregg RG, Peachey NS (2002) Elimination of the ρ1 subunit abolishes $GABA_C$ receptor expression and alters visual processing in the mouse retina. J Neurosci 22(10):4163–4174

Nirenberg S, Meister M (1997) The light response of retinal ganglion cells is truncated by a displaced amacrine circuit. Neuron 18(4):637–650

Parzen E (1962) On estimation of a probability density function and mode. Ann Math Stat 33(3):1065–1076

Popova E, Mitova L, Vitanova L, Kupenova P (2003) Effect of GABAergic blockade on light responses of frog retinal ganglion cells. Comp Biochem Physiol C 134(2):175–187

Protti DA, Gerschenfeld HM, Llano I (1997) GABAergic and glycinergic IPSCs in ganglion cells of rat retinal slices. J Neurosci 17(16):6075–6085

Rosenblatt M (1956) Remarks on some nonparametric estimates of a density function. Ann Math Stat 27(3):832–837

Roska B, Nemeth E, Werblin FS (1998) Response to change is facilitated by a three-neuron disinhibitory pathway in the tiger salamander retina. J Neurosci 18(9):3451–3459

Shen W, Jiang Z (2007) Characterization of glycinergic synapses in vertebrate retinas. J Biomed Sci 14(1):5–13. doi:10.1007/s11373-006-9118-2

Soucy ED, Wang Y-S, Nirenberg S, Nathans J, Meister M (1998) A novel signaling pathway from rod photoreceptors to ganglion cells in mammalian retina. Neuron 21(3):481–493

Thiel A, Greschner M, Ammermüller J (2006) The temporal structure of transient ON/OFF ganglion cell responses and its relation to intra-retinal processing. J Comput Neurosci 21(2):131–151. doi:10.1007/s10827-006-7863-x

Toychiev AH, Yee CW, Sagdullaev BT (2013) Correlated spontaneous activity persists in adult retina and is suppressed by inhibitory inputs. PLoS One 8(10):e77658

Van Wyk M, Taylor WR, Vaney DI (2006) Local edge detectors: a substrate for fine spatial vision at low temporal frequencies in rabbit retina. J Neurosci 26(51):13250–13263

Venkataramani S, Van Wyk M, Buldyrev I, Sivyer B, Vaney DI, Taylor WR (2014) Distinct roles for inhibition in spatial and temporal tuning of local edge detectors in the rabbit retina. PLoS One 9(2):e88560

Wässle H (2004) Parallel processing in the mammalian retina. Nat Rev Neurosci 5(10):747–757. doi:10.1038/nrn1497

Wässle H, Koulen P, Brandstätter JH, Fletcher EL, Becker C-M (1998) Glycine and GABA receptors in the mammalian retina. Vis Res 38(10):1411–1430

Wässle H, Heinze L, Ivanova E, Majumdar S, Weiss J, Harvey RJ, Haverkamp S (2009) Glycinergic transmission in the mammalian retina. Front Mol Neurosci. doi:10.3389/neuro.02.006.2009

Werblin FS (2011) The retinal hypercircuit: a repeating synaptic interactive motif underlying visual function. J Physiol 589(15):3691–3702. doi:10.1113/jphysiol.2011.210617

Xu Y, Dhingra NK, Smith RG, Sterling P (2005) Sluggish and brisk ganglion cells detect contrast with similar sensitivity. J Neurophysiol 93(5):2388–2395. doi:10.1152/jn.01088.2004

Yang X-L (2004) Characterization of receptors for glutamate and GABA in retinal neurons. Prog Neurobiol 73(2):127–150. doi:10.1016/j.pneurobio.2004.04.002

Zhang J, Jung C-S, Slaughter MM (1997) Serial inhibitory synapses in retina. Vis Neurosci 14(03):553–563

Zhang P-M, Wu J-Y, Zhou Y, Liang P-J, Yuan J-Q (2004) Spike sorting based on automatic template reconstruction with a partial solution to the overlapping problem. J Neurosci Methods 135(1):55–65. doi:10.1016/j.jneumeth.2003.12.001

Zhang Y-Y, Wang R-B, Pan X-C, Gong H-Q, Liang P-J (2014) Visual pattern discrimination by population retinal ganglion cells' activities during natural movie stimulation. Cogn Neurodyn 8(1):27–35. doi:10.1007/s11571-013-9266-9

Zhou Y, Liu X, Liang P-J (2007) The dual-peak light response of ganglion cells in chicken retina. Brain Res 1138:104–110. doi:10.1016/j.brainres.2006.12.070